

OAMixer: Object-aware Mixing Layer for Vision Transformers

Hyunwoo Kang* Sangwoo Mo* Jinwoo Shin
KAIST

{hyunwookang, swmo, jinwoos}@kaist.ac.kr

Abstract

Patch-based models, e.g., Vision Transformers (ViTs) and Mixers, have shown impressive results on various visual recognition tasks, alternating classic convolutional networks. While the initial patch-based models (ViTs) treated all patches equally, recent studies reveal that incorporating inductive bias like spatiality benefits the representations. However, most prior works solely focused on the location of patches, overlooking the scene structure of images. Thus, we aim to further guide the interaction of patches using the object information. Specifically, we propose OAMixer (object-aware mixing layer), which calibrates the patch mixing layers of patch-based models based on the object labels. Here, we obtain the object labels in unsupervised or weakly-supervised manners, i.e., no additional human-annotating cost is necessary. Using the object labels, OAMixer computes a reweighting mask with a learnable scale parameter that intensifies the interaction of patches containing similar objects and applies the mask to the patch mixing layers. By learning an object-centric representation, we demonstrate that OAMixer improves the classification accuracy and background robustness of various patch-based models, including ViTs, MLP-Mixers, and ConvMixers. Moreover, we show that OAMixer enhances various downstream tasks, including large-scale classification, self-supervised learning, and multi-object recognition, verifying the generic applicability of OAMixer.¹

1. Introduction

Patch-based models, i.e., models that process an input image as a sequence of visual patches, have arisen as a new paradigm of neural networks for visual data, regarded as a promising alternative to convolutional neural networks (CNNs) [31]. Remarkably, patch-based models have achieved state-of-the-art results on various computer vision tasks by favoring the scaling properties [1, 19, 61]. Moreover, patch-based models merit multiple advantages,

including out-of-distribution generalization [4, 37, 39], a natural extension to video domains [3, 5], integration with other domains like language or speech [2, 40], and easily combined with state-of-the-art visual self-supervised learning [22].

The core concept of patch-based models is to update patch-wise representations by alternating the computation *within* patches and *among* patches, called channel mixing and patch (or token) mixing, respectively. To this end, the design of patch mixing layers is widely investigated. The pioneering work named Vision Transformer (ViT) [19] considered self-attention [49], and other works considered various mixing layers such as feed-forward [33, 45, 46], convolution [48], or even pooling operation [57]. Most standard patch-based models use self-attention or feed-forward mixing layers, which minimizes the prespecified inductive biases by employing all patches equally [28].

While this data-centric approach is effective in large-scale scenarios, recent works claim that incorporating inductive biases is still vital for patch-based models, especially when learned from limited data [44]. To this end, numerous works incorporated spatial inductive bias for patch-based models following the analogy of convolutions. They can be categorized into two groups: designing a patch mixing layer utilizing the location of patches [15, 16, 32, 48, 53] or building an architecture that combines convolutional or pooling layers with patch mixing layers [20, 25, 34, 52, 56, 58, 59]. However, both approaches focus on sample-agnostic spatial inductive bias, which overlooks the sample-specific object structures.

Contribution. We propose OAMixer, a novel reweighting scheme for patch mixing layers leveraging the object structure of images. The main idea of OAMixer is to strengthen the interaction of patches containing similar objects while regularizing the connection of different objects (and background). Intuitively, OAMixer improves the discriminability of objects (i.e., better classification) and reduces the spurious correlations between objects and backgrounds (i.e., robust to background shifts) by disentangling object representations. Figure 1 visualizes the high-level concept of OAMixer.

*Equal contribution

¹Code: <https://github.com/alinelab/OAMixer>

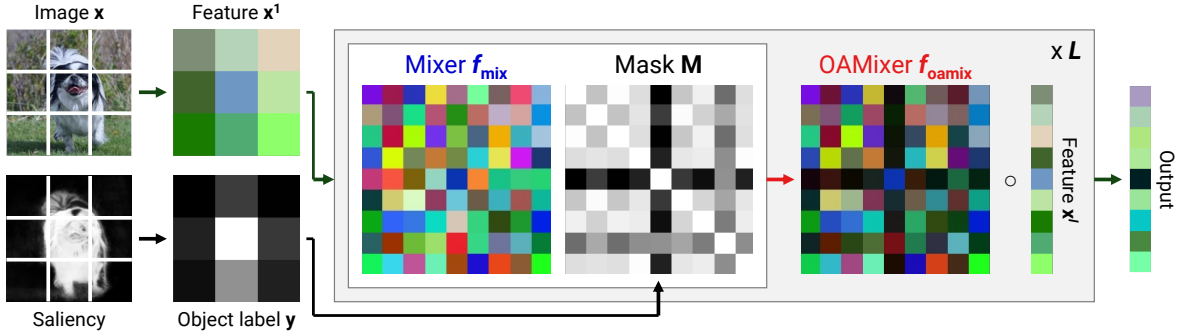


Figure 1. Conceptual illustration of our method, OAMixer. Given an image x , we assume that patch-wise object labels y (either from pixel-level labels or given by patch-level directly) are available. Using this label, we compute a reweighting mask M which modifies the original patch mixing layer f_{mix} to the data-specific *object-aware mixed* layer f_{oamix} .

Our framework consists of two stages. First, we compute a reweighting mask for each image using the pairwise similarity of patches, where patch-wise object labels give the similarity. Here, one can obtain the object labels in unsupervised or weakly-supervised manners, i.e., no additional human-annotating cost is necessary.² We then calibrate the interaction of patch mixing layers using the reweighting mask and a learnable scale parameter that controls the level of calibration. Although OAMixer can be applied to any patch-based model in principle, one needs a careful design to consider the interaction dynamics of each layer. Thus, we illustrate specific instantiations of OAMixer for three representative mixing layers: self-attention, feed-forward, and convolution.

In our experiments, we demonstrate the superiority of object-aware inductive bias from OAMixer:

- Improves classification and background robustness over various patch-based models, including ViTs [19], MLP-Mixers [45], and ConvMixers [48].
- Outperforms the patch mixing layers considering spatial inductive bias (e.g., ConViT [16]).
- Outperforms the prior methods utilizing patch-level supervision (e.g., TokenLabeling [27]).
- Unlike prior methods (e.g., ConViT and TokenLabeling), OAMixer enhances the background robustness.

OAMixer also benefits various downstream tasks:

- Improves large-scale classification, e.g., increases ImageNet [17] top-1 accuracy of DeiT-B [47] from 78.45% to 82.18% (+3.73%).
- Improves self-supervised learning, e.g., increases ImageNet linear probing of DeiT-T with DINO [11] from 59.37% to 61.16% (+1.79%).

²One can also use a pretrained object labeler trained on some external dataset like ImageNet.

2. Related work

Patch-based models. Inspired by the success of Transformers (or self-attention) [49] in natural language processing [10, 18], numerous works have attempted to extend Transformers for computer vision [28]. In particular, the seminal work named Vision Transformer (ViT) [19] discovered that Transformer could achieve state-of-the-art performance, alternating convolutional neural networks (CNNs) [31]. Other studies revealed that different patch mixing layers such as feed-forward [45], convolution [48], or even a pooling operation [57] are comparable to self-attention, hypothesizing that the success of ViT comes from the patch-based architectures. Our work proposes a universal framework to improve the patch-based models by introducing object-aware inductive bias to their patch mixing layers.

Inductive bias for patch-based models. Many patch-based models aim to remove inductive biases by using patch mixing layers without additional structures, e.g., self-attention. While they perform well on large data regimes, recent works reveal that inductive biases are still crucial for patch-based models, especially under limited data [44]. Consequently, extensive literature proposed approaches to incorporate additional structures for patch-based models, e.g., spatial structures of CNNs. One line of work aims to design patch mixing layers reflecting inductive biases. For example, ConViT [16] and CoAtNet [15] calibrate self-attention with spatial distances between patches, CvT [53] and ConvMixer [48] utilize convolution operation for patch mixing. Another line of work builds an architecture that combines convolutional or pooling layers with patch mixing layers [20, 25, 34, 52, 56, 58, 59]. Our work falls into the first category; however, we leverage the object structure of images, unlike prior works that focus on the spatial inductive bias. Using rich object information, our proposed OAMixer outperforms ConViT and CoAtNet, and using both gives further improvements, i.e., two methods con-

tribute to the model differently (see Table 1). We also emphasize that OAMixer can be applied to any patch mixing layers under a common principle, unlike prior works designed for specific layers.

Incorporating object structures. Although objects are the atom of scenes, only a limited number of research has leveraged the object structure of images for visual recognition.³ This is mainly due to two reasons: (a) the cost of object labels and (b) the non-triviality of reflecting object structure in neural networks. Recently, both challenges have been relaxed. First, the advance of unsupervised [11, 36, 50] and weakly-supervised [12, 43, 60] saliency detection significantly reduced the labeling cost of objects. Specifically, we use BigBiGAN [50] and ReLabel [60] object labels in our experiments; no human annotations are required. Second, patch-based models are well-suited with object labels since the reduced resolution of patches (e.g., 16×16 patches instead of 224×224 pixels) enables the computation of their relations. OAMixer reflects the object structures into patch-based models in favor of these two advances. ORViT [26] directs video Transformers to focus on object regions, but they are less suited for image recognition. TokenLabeling [27] uses patch labels for auxiliary objectives; it can be combined with OAMixer and gives orthogonal gain (see Table 1). We finally note that several works [29, 35, 54] aim to disentangle the object representation explicitly. However, they do not scale yet to complex real-world images due to the strong constraints in the model. In contrast, OAMixer can be applied to any existing patch-based models with minimal modification.

3. OAMixer: Object-aware Mixing Layer

We first introduce OAMixer, an object-aware mixing layer for patch-based models in Section 3.1. We then illustrate the instantiations of OAMixer on various mixing layers in Section 3.2. Finally, we discuss strategies to obtain patch-wise labels efficiently (e.g., unsupervised) in Section 3.3.

3.1. Computing reweighting mask for OAMixer

The idea of patch-based models is to reshape a 2D image $\mathbf{x} \in \mathbb{R}^{H \times W \times C}$ into a sequence of flattened 2D patches $\mathbf{x}^0 \in \mathbb{R}^{N \times (P^2 C)}$, where (H, W) is the resolution of original image, C is the number of color channels, (P, P) is the resolution of each image patch, and $N = HW/P^2$ is the number of patches. Patch-based models first convert the 2D patches into patch (or token) features $\mathbf{x}^1 := f_{\text{embed}}(\mathbf{x}^0) \in \mathbb{R}^{N \times D}$ with latent dimension D using an embedding function f_{embed} , then update the patch features by alternating two operations: (a) patch mixing layers $f_{\text{mix}}^l : \mathbb{R}^N \rightarrow \mathbb{R}^N$

³Some prior work [13, 14] considered objects to modify features, but they simply masked the non-object regions, which loses information. We also tried a similar approach, but soft masking performed better.

which mix the features among patches, and (b) channel mixing layers $g_{\text{mix}}^l : \mathbb{R}^D \rightarrow \mathbb{R}^D$ which mix the features among channels, where l implies the operation of layer l . Formally, the l -th layer of patch-based model updates an input vector $\mathbf{x}^l \in \mathbb{R}^{N \times D}$ to an output vector $\mathbf{x}^{l+1} \in \mathbb{R}^{N \times D}$ following:

$$\mathbf{z}^{l+1} = [\mathbf{z}_{1:N,d}^{l+1}] = [f_{\text{mix}}(\mathbf{x}_{1,d}^l; \mathbf{x}_{2,d}^l; \dots; \mathbf{x}_{N,d}^l)] \quad (1)$$

$$\mathbf{x}^{l+1} = [\mathbf{x}_{n,1:D}^{l+1}] = [g_{\text{mix}}(\mathbf{z}_{n,1}^{l+1}; \mathbf{z}_{n,2}^{l+1}; \dots; \mathbf{z}_{n,D}^{l+1})] \quad (2)$$

where $\mathbf{z}_{n,d}$ and $\mathbf{x}_{n,d}$ denotes n -th patch, d -th channel value, and $\mathbf{z}_{1:N,d}^{l+1} \in \mathbb{R}^N$ and $\mathbf{x}_{n,1:D}^{l+1} \in \mathbb{R}^D$ denotes row-wise and column-wise subvector of \mathbf{z} and \mathbf{x} , respectively.

We introduce OAMixer, a universal framework for improving patch mixing layers f_{mix} by incorporating the object structure of images. With the object information, OAMixer strengthens the interaction of patches of similar objects while regularizing the connection of different objects and backgrounds. To this end, we utilize the patch-wise labels $\mathbf{y} \in \mathbb{R}^{N \times K}$ where K is the number of object classes. Using them, we compute the reweighting mask $\mathbf{M}^l \in \mathbb{R}^{N \times N}$, a patch-wise semantical similarity mask. Formally, we set the (i, j) -th value of the reweighting mask \mathbf{M}_{ij}^l as a reverse distance between the object labels of two patches \mathbf{y}_i and \mathbf{y}_j :

$$\mathbf{M}_{ij}^l := \exp(-\kappa^{(l)} \cdot d(\mathbf{y}_i, \mathbf{y}_j)) \in (0, 1] \quad (3)$$

where $\kappa^{(l)} \geq 0$ is a learnable mask scale (scalar) parameter for each layer and $d(\cdot, \cdot) : \mathbb{R}^K \times \mathbb{R}^K \rightarrow \mathbb{R}$ is a distance function for object labels. We initialize $\kappa^{(l)}$ by zero for training, i.e., consider the full interaction initially then focus on the objects as $\kappa^{(l)}$ increases. We observe that the model sets higher $\kappa^{(l)}$ for lower layers and lower $\kappa^{(l)}$ for higher layers after training, i.e., OAMixer automatically attends the intra-object relations first then expand to the inter-object relations, which resembles the structure of CNNs (see Table 7).

We calibrate the $N \times N$ interaction of patch mixing layers using the reweighting mask \mathbf{M} . If the patch mixing layer $f_{\text{mix}} := \mathbf{L}_{\text{mix}}$ is linear, one can simply (element-wise) multiply the mask to get OAMixer; $\mathbf{M} \odot \mathbf{L}_{\text{mix}}$. While OAMixer can be applied to any patch layers in principle, one needs careful design to consider the nonlinear dynamics of each layer. We provide specific implementations of OAMixer on various representative models in the next section.

3.2. OAMixer for ViT and Mixers

We briefly review three representative patch mixing layers: self-attention, feed-forward, and convolution, and describe the implementations of OAMixer for each layer.

OAMixer for self-attention. Self-attention [49] mixing layers update patch features by aggregating values with nor-

malized importances (or attentions):

$$f_{\text{mix}}(\mathbf{x}) := \underbrace{\text{Softmax}\left(\frac{\mathbf{Q}\mathbf{K}^T}{\sqrt{D_K}}\right)}_{\text{attention matrix } \mathbf{A}} \cdot \mathbf{V} \quad (4)$$

where \mathbf{Q} , \mathbf{K} , \mathbf{V} are query, key, and value, respectively, which are linear projections of input $\mathbf{x} \in \mathbb{R}^{N \times D}$, given by $\mathbf{Q} := \mathbf{x} \cdot \mathbf{W}_Q \in \mathbb{R}^{N \times D_K}$, $\mathbf{K} := \mathbf{x} \cdot \mathbf{W}_K \in \mathbb{R}^{N \times D_K}$, and $\mathbf{V} := \mathbf{x} \cdot \mathbf{W}_V \in \mathbb{R}^{N \times D_V}$. Here, we compute H independent attention heads and aggregate outputs for the final output of size $N \times D$ for $D = H \cdot D_V$. Recall that self-attention is basically a matrix multiplication of attention \mathbf{A} and value \mathbf{V} matrices, and one can (element-wise) multiply the reweighting mask \mathbf{M} to the attention matrix to calibrate interaction. Then, we renormalize the masked attention $\mathbf{M} \odot \mathbf{A}$ to make the row-wise sum be 1 as the original self-attention. To sum up, OAMixer for self-attention is:

$$f_{\text{oamix}}(\mathbf{x}) := [\tilde{\mathbf{A}}_{ij}] \cdot \mathbf{V} = \left[\frac{\mathbf{M}_{ij} \cdot \mathbf{A}_{ij}}{\sum_j \mathbf{M}_{ij} \cdot \mathbf{A}_{ij}} \right] \cdot \mathbf{V} \quad (5)$$

where $\tilde{\mathbf{A}}$ is the renormalized masked attention. We finally remark that patch-based models using self-attention often use the additional [CLS] token to aggregate the global feature. Here, we define the mask value between the [CLS] token and every other patch to be one and apply Eq. (5).

OAMixer for feed-forward. Feed-forward (or multi-layer perceptron; MLP) mixing layers update patch features with a channel-wise MLP. Since each channel is computed independently, we only consider a $N \times 1$ vector of a single channel. Then, the mixer layer is:

$$f_{\text{mix}}(\mathbf{x}) := \mathbf{W}_m \cdot \sigma(\mathbf{W}_{m-1} \cdot \sigma(\cdots \sigma(\mathbf{W}_1 \cdot \mathbf{x}))) \quad (6)$$

where $\mathbf{W}_1, \dots, \mathbf{W}_m$ are weight matrices and σ is a non-linear activation. However, it is nontrivial to apply the reweighting mask \mathbf{M} since f_{mix} is nonlinear. To tackle this issue, we decompose the mixing layer f_{mix} into a linear approximation $\mathbf{L}_{\text{mix}}^{\mathbf{x}} \cdot \mathbf{x} \approx f_{\text{mix}}(\mathbf{x})$ for a (possibly data-dependent) matrix $\mathbf{L}_{\text{mix}}^{\mathbf{x}} \in \mathbb{R}^{N \times N}$ and a residual term $f_{\text{mix}}(\mathbf{x}) - \mathbf{L}_{\text{mix}}^{\mathbf{x}} \cdot \mathbf{x}$. Here, we only calibrate the linear term but omit the residual term. Then, OAMixer for feed-forward is given by:

$$f_{\text{oamix}}(\mathbf{x}) := \underbrace{(\mathbf{M} \odot \mathbf{L}_{\text{mix}}^{\mathbf{x}})}_{\text{masked linear}} \cdot \mathbf{x} + \underbrace{(f_{\text{mix}}(\mathbf{x}) - \mathbf{L}_{\text{mix}}^{\mathbf{x}} \cdot \mathbf{x})}_{\text{residual}} \quad (7)$$

where \odot is an element-wise product. While finding a good $\mathbf{L}_{\text{mix}}^{\mathbf{x}}$ is nontrivial in general, we found that simply dropping nonlinear activations gives an efficient yet effective solution:

$$\mathbf{L}_{\text{mix}} := \mathbf{W}_m \mathbf{W}_{m-1} \cdots \mathbf{W}_1 \in \mathbb{R}^{N \times N}. \quad (8)$$

We observe that this (somewhat crude) approximation performs well. We also tried some data-dependent variants but did not see gain despite their computational burdens.

OAMixer for convolution. Convolutional mixing layers update patch features with a channel-wise 2D convolution. Similar to the feed-forward case, we only consider a single channel input \mathbf{x} (which is $\mathbf{x}_{1:N,d}$ formally), reshaped as a $1 \times \bar{H} \times \bar{W}$ tensor where $(\bar{H}, \bar{W}) = (H/P, W/P)$ is the resolution of patch features. Then, the mixer layer is:

$$f_{\text{mix}}(\mathbf{x}) := \mathbf{W}_{\text{conv}} * \mathbf{x} \quad (9)$$

where $\mathbf{W}_{\text{conv}} \in \mathbb{R}^{1 \times 1 \times S \times S}$ is a kernel matrix with size S and $*$ denotes convolution operation. Here, we consider the linearized version of kernel matrix (i.e., Toeplitz matrix) that substitutes the convolution to the matrix multiplication. Then, one can interpret the mixer layer as:

$$f_{\text{mix}}(\mathbf{x}) = \mathbf{W}_{\text{linear}} \cdot \tilde{\mathbf{x}} \quad (10)$$

where $\mathbf{W}_{\text{linear}} \in \mathbb{R}^{N \times N}$ is the corresponding matrix of \mathbf{W}_{conv} and $\tilde{\mathbf{x}}$ is a reshaped tensor of \mathbf{x} of size $N \times 1$, where $N = \bar{H} \cdot \bar{W}$. Here, one can directly multiply the reweighting mask \mathbf{M} to define the OAMixer for convolution:

$$f_{\text{oamix}}(\mathbf{x}) := (\mathbf{M} \odot \mathbf{W}_{\text{linear}}) \cdot \tilde{\mathbf{x}} \quad (11)$$

where \odot is an element-wise product. We also compare OAMixer with the models using different kernel matrix for each channel, i.e., $\mathbf{W}_{\text{conv}} \in \mathbb{R}^{D \times 1 \times S \times S}$ (see Appendix E).

3.3. Obtaining object labels

One possible concern on OAMixer is the annotation cost of object labels $\mathbf{y} \in \mathbb{R}^{N \times K}$. To alleviate this issue, we leverage the recent advances in unsupervised and weakly-supervised saliency detection. Specifically, we consider a two-stage training: train an object labeler on the downstream dataset, then train a OAMixer model (on the same dataset) using the object labeler. Here, one can also use an object labeler pretrained under some external dataset like ImageNet [17], instead of training a new object labeler for each downstream dataset.⁴ In the remaining section, we recap the two types of machine annotators: binary saliency and multi-class prediction, and discuss their pros and cons.

Binary saliency map. We first consider binary saliency maps, i.e., indicating whether the given pixel is an object or background. There is a tremendous amount of work on inferring saliency maps in unsupervised [11, 36, 50] or weakly-supervised (i.e., using class labels) [12, 43] manners. We use an unsupervised method called BigBiGAN [50], which finds the salient region using the latent space of BigGAN [9]. We also use the attention map of pretrained

⁴The newly trained and ImageNet-pretrained object labelers show comparable performance in our experiments (see Table 5).

Table 1. Comparison of various scenarios evaluated on the Background Challenge benchmark. We report the classification accuracy (\uparrow) and background robustness (\downarrow), where higher and lower values are better for each metric. ‘‘TL’’ indicates TokenLabeling, that the model is trained with an additional token-level objective. Note that TL improves the overall performance; we colored them with gray lines for better visualization. We use ReLabel from ImageNet trained model for both OAMixer and TL. ‘+’ denotes the modules added to the baseline (not accumulated), and parenthesis denotes the gap from the baseline. The table has several implications: (a) OAMixer consistently improves the classification and background robustness, confirming the benefit of object-centric representation. (b) OAMixer outperforms the methods using spatial inductive bias like ConViT and CoAtNet; combining ConViT and OAMixer performs even better. (c) OAMixer gives additional gain over TL, verifying the merit of guided patch interaction over naive patch-level objective. (d) OAMixer also improves MLP-Mixer and ConvMixer, patch-based models using different patch mixing layers.

	TL	Original (\uparrow)	Only-BG-B (\downarrow)	Mixed-Same (\uparrow)	Mixed-Rand (\uparrow)	BG-Gap (\downarrow)
DeiT-T	-	70.62	35.48	63.31	39.56	23.75
+ ConViT	-	78.74 (+8.12)	38.69 (+3.21)	70.84 (+7.53)	46.91 (+7.35)	23.93 (+0.18)
+ CoAtNet	-	78.62 (+8.00)	37.68 (+2.20)	70.40 (+7.09)	45.46 (+5.90)	24.94 (+1.19)
+ OAMixer (ours)	-	81.98 (+11.36)	30.89 (-4.59)	73.38 (+10.07)	51.53 (+11.97)	21.85 (-1.90)
+ OAMixer + ConViT (ours)	-	83.38 (+12.76)	31.36 (-4.12)	74.86 (+11.55)	53.14 (+13.58)	21.73 (-2.02)
DeiT-T	\checkmark	83.50	37.01	74.57	51.78	22.79
+ OAMixer (ours)	\checkmark	87.23 (+3.73)	29.21 (-7.80)	78.15 (+3.58)	60.59 (+8.81)	17.56 (-5.23)
DeiT-S	-	82.69	39.46	73.88	50.49	23.39
+ ConViT	-	85.51 (+2.82)	38.94 (-0.52)	76.40 (+2.52)	54.37 (+3.88)	22.03 (-1.36)
+ OAMixer (ours)	-	86.32 (+3.63)	31.78 (-7.68)	78.44 (+4.56)	56.74 (+6.25)	21.70 (-1.69)
+ OAMixer + ConViT (ours)	-	88.20 (+5.51)	30.79 (-8.67)	79.16 (+5.28)	60.52 (+10.03)	18.64 (-4.75)
DeiT-S	\checkmark	88.52	38.00	79.43	59.36	20.07
+ OAMixer (ours)	\checkmark	91.31 (+2.79)	29.19 (-8.81)	81.78 (+2.35)	66.92 (+7.56)	14.86 (-5.21)
MLP-Mixer-S/16	-	84.99	40.96	76.52	54.72	21.80
+ OAMixer (ours)	-	87.68 (+2.69)	27.28 (-13.68)	79.43 (+2.91)	60.44 (+5.72)	18.99 (-2.81)
MLP-Mixer-S/16	\checkmark	88.07	38.17	79.21	58.72	20.49
+ OAMixer (ours)	\checkmark	90.49 (+2.42)	28.72 (-9.45)	81.63 (+2.42)	65.36 (+6.64)	16.27 (-4.22)
ConvMixer-S/16	-	86.32	41.38	78.59	56.99	21.60
+ OAMixer (ours)	-	88.49 (+2.17)	35.60 (-5.78)	81.70 (+3.11)	63.93 (+6.94)	17.77 (-3.83)
ConvMixer-S/16	\checkmark	87.49	36.49	80.42	58.15	22.27
+ OAMixer (ours)	\checkmark	89.09 (+1.60)	32.67 (-3.82)	82.64 (+2.22)	63.70 (+5.55)	18.94 (-3.33)

DINO [11] model to extract the object information unsupervised. From the binary saliency map, we get a soft label $y_n \in [0, 1]$, and use the l_1 -distance between the object labels of two patches in Eq. (3).

Multi-class prediction map. We also consider multi-class prediction maps, i.e., pixel- or patch-level semantic masks. In particular, we use ReLabel [60], a weakly-supervised method that predicts dense label maps from an image classifier by applying the classifier to the penultimate spatial features (i.e., before global average pooling). We then resize the label map (by pooling over interpolated values) to match the resolution of tokens and get the object labels $y_n \in \mathbb{R}^K$. Here, we use the cosine distance to compute the distance between object labels of two patches.

Comparison of two approaches. Multi-class prediction map contains richer semantics and thus provides more informative reweighing masks. As a result, OAMixer using ReLabel performs better than BigBiGAN in most cases.

In particular, we use multi-class prediction maps for multi-object images since binary saliency maps cannot distinguish different objects. However, BigBiGAN works better on distribution shifts, as finding salient regions is easier than predicting semantics for the unseen images. Thus, the users can choose binary or multi-class labels on their purpose.

4. Experiments

We first show that the object-centric design (i.e., disentangled representation of objects and background) of OAMixer improves the classification accuracy and background robustness of various patch-based models in Section 4.1. We then verify the applicability of OAMixer over various downstream tasks, including large-scale classification, self-supervised learning, and multi-object recognition in Section 4.2. We finally provide analyses in Section 4.3.

Models and training. We apply OAMixer on three representative patch-based models: DeiT [47], MLP-Mixer

Table 2. ImageNet top-1 accuracy. We add TokenLabeling (TL) and OAMixer on top of the baseline models (accumulated). Both TL and OAMixer use ReLabel object labels from ImageNet-trained model. Bold denotes the best result, and parenthesis denotes the gap from the baseline. Note that TL requires enough model capacity (better for the larger model, even harms MobileViT-XXS). In contrast, OAMixer gives a consistent improvement over all considered model capacities.

	MobileViT-XXS	DeiT-T	DeiT-S	DeiT-B
# params	1.3M	5M	22M	86M
Baseline	62.56	71.19	79.30	78.45
+ TokenLabeling	62.34 (-0.22)	71.61 (+0.42)	80.20 (+0.90)	81.17 (+2.72)
+ OAMixer (ours)	64.78 (+2.22)	74.26 (+3.07)	81.26 (+1.96)	82.18 (+3.73)

Table 3. Linear probing results of DINO with DeiT-T trained on ImageNet with 100 epochs. We use the unsupervised attention map from the pretrained baseline DINO model as a patch-wise object label for OAMixer. We test the in-domain accuracy with the ImageNet validation dataset and out-domain accuracy with Background Challenge datasets after training the linear classifier on the ImageNet train set with 100 epochs. The results show that OAMixer is effective in the self-supervised framework.

	ImageNet (↑)	Only-BG-B (↓)	Mixed-Same (↑)	Mixed-Rand (↑)	BG-Gap (↓)
DeiT-T	59.37	34.27	89.73	78.07	11.66
+ OAMixer	61.16 (+1.79)	20.20 (-14.07)	89.75 (+0.02)	79.33 (+1.26)	10.42 (-1.24)

[45], and ConvMixer [48], using self-attention, feed-forward, and convolutional patch mixing layers, respectively. Specifically, we use DeiT-T, DeiT-S, MLP-Mixer-S/32, and MLP-Mixer-S/16 configurations. For ConvMixer, we follow the configuration of MLP-Mixer (dim: 512, depth: 8) and use kernel size of 9 for a fair comparison with MLP-Mixer. We denote these variants as ConvMixer-S/32 and ConvMixer-S/16. We share the convolution kernel over channels by default, while we provide the unshared results in Appendix E. We follow the default training setup of DeiT, but use a batch size of 256 due to GPU memory issue.

Object labels. We consider binary and multi-class prediction maps, as explained in Section 3.3. The object labels are either trained on each downstream dataset or pretrained on ImageNet [17]. We train a ResNet-18 [23] network to obtain ReLabel on the downstream dataset and use the BigBiGAN and ReLabel with NFNet-F6 [8] trained on the ImageNet dataset for pretrained object labelers.

4.1. Main results

In this section, we show that the object-aware inductive bias from OAMixer improves classification and background robustness over various patch-based models. To this end, we conduct experiments on the Background Challenge [55] benchmark, which consists of a smaller (9 superclass, 370 class) subset of ImageNet as a training dataset, called ImageNet-9 (IN-9), and eight test datasets to evaluate the classification and background robustness.⁵ In this section,

⁵We also provide the results using a larger version of IN-9 (IN-9L) as a training dataset in Appendix D. It improves the overall performance of all models but shows a similar tendency with IN-9.

we will demonstrate that (a) OAMixer improves classification and background robustness over various patch-based models, OAMixer outperforms (b) prior methods using spatial inductive bias, and (c) prior methods using patch-level supervision. In addition, we compare OAMixer using different object labels including BigBiGAN in Appendix B.

Setup. Background Challenge contains eight evaluation datasets with different combinations of foregrounds and backgrounds: ORIGINAL (↑), ONLY-BG-B (↓), ONLY-BG-T (↓), NO-FG (↓), ONLY-FG (↑), MIXED-SAME (↑), MIXED-RAND (↑), MIXED-NEXT (↑), where the upper or lower arrows imply the model should predict the class well or not, respectively. Namely, the model should increase the accuracy of (↑) datasets while decrease the accuracy (or increase the background robustness) of (↓) datasets. We also report BG-GAP (↓) which measures the accuracy gap between MIXED-SAME and MIXED-RAND. We omit ONLY-BG-T, NO-FG, ONLY-FG, and MIXED-NEXT results for the brevity (see Appendix A for discussion). We use ReLabel trained on ImageNet in the experiments, but ReLabel trained on IN-9 gives similar trends (see Appendix C).

Classification and background robustness. Table 1 presents the results on the Background Challenge benchmark, which has several additional implications that will be discussed in a few following paragraphs. First, we remark that OAMixer consistently improves the classification and background robustness in all considered patch-based models. To highlight a few numbers, OAMixer enhances the classification accuracy of DeiT-T from 70.62% to 81.98% (+11.36%) on the ORIGINAL dataset while reducing the background bias of MLP-Mixer-S/16 from

Table 4. Classification accuracy on various distribution-shifted datasets. Bold denotes the best results, and parenthesis denotes the gap from the baseline. OAMixer gives consistent improvements.

	ImageNet-9	ImageNetV2-9	Real-9	Rendition-9	Stylized-9	Sketch-9
DeiT-T	70.62	63.19	68.13	24.14	16.66	21.65
+ OAMixer (ours)	80.15 (+9.53)	70.68 (+7.49)	77.78 (+9.65)	27.53 (+3.39)	21.80 (+5.14)	24.45 (+2.80)
DeiT-S	82.69	73.22	80.21	28.60	21.90	27.26
+ OAMixer (ours)	83.88 (+1.19)	75.68 (+2.46)	82.37 (+2.16)	29.43 (+0.83)	24.64 (+2.74)	27.93 (+0.67)

Table 5. Classification accuracy on various datasets. We add OAMixer to the baseline models, where ‘‘OAMixer’’ uses ReLabel trained on each downstream dataset, and ‘‘OAMixer*’’ uses ReLabel trained on ImageNet. Bold denotes the best result among methods not using ImageNet data (not colored by gray lines), and parenthesis denotes the gap from the baseline. OAMixer gives a consistent improvement, showing comparable results with OAMixer* for all considered datasets.

	DeiT-T			DeiT-S		
	Baseline	OAMixer (ours)	OAMixer* (ours)	Baseline	OAMixer (ours)	OAMixer* (ours)
CIFAR-10	86.35	89.89 (+3.54)	88.09 (+1.74)	90.80	92.73 (+1.93)	92.33 (+1.53)
CIFAR-100	65.21	66.94 (+1.73)	67.21 (+2.00)	70.08	71.00 (+0.92)	71.63 (+1.55)
Food-101	69.83	72.25 (+2.42)	71.50 (+1.67)	75.00	75.17 (+0.17)	76.03 (+1.03)
Pets	24.20	24.50 (+0.30)	24.97 (+0.57)	25.57	30.64 (+5.07)	29.63 (+4.06)

40.96% to 27.28% (-13.68%) on the ONLY-BG-B dataset. These results support that OAMixer learns more object-centric representation robust to background shifts.

Comparison with methods using spatial inductive bias. We compare OAMixer with patch mixing layers using spatial inductive bias: ConViT [16] and CoAtNet [15]. We only take the modified self-attention layers from both models and apply them to DeiT for a fair comparison with OAMixer. ConViT and CoAtNet calibrate the self-attention but use spatial distance instead of semantic distance from object labels. We keep the last two layers of ConViT as the vanilla self-attention following the original paper. Table 1 shows that OAMixer outperforms both ConViT and CoAtNet for all considered scenarios. Notably, the DeiT-T results show that spatial inductive bias often does not help background robustness, as local aggregation does not prevent the entangling of patches in adjacent regions. We also remark that combining ConViT and OAMixer performs the best; they give orthogonal benefits.

Comparison with methods using patch-level supervision. We compare OAMixer with prior work using patch-level supervision, TokenLabeling (TL) [27]. Specifically, TL uses the object (or patch) labels as an additional objective for each patch. We remark that TL and OAMixer benefit the model differently, and using both performs the best. Table 1 shows that OAMixer+TL outperforms TL for all considered scenarios. It confirms that the advantage of OAMixer comes from the guided patch interaction, not only from the usage of patch-level supervision. In particular, we highlight that TL does not improve the background robust-

ness, unlike OAMixer gives a significant gain.

4.2. Various downstream tasks

In this section, we verify the benefits of OAMixer on various computer vision tasks, including ImageNet classification, self-supervised learning, and multi-object recognition. To do so, we conduct experiments on the ViT and apply OAMixer on self-attention since ViTs are the most widely used patch-based models in various applications.

ImageNet classification. Table 2 presents the ImageNet [17] top-1 accuracy of OAMixer and baseline models on various ViT architectures: MobileViT and DeiT. For a fair comparison, we also compare OAMixer with TokenLabeling (TL) [27], which also uses object labels for training. We use ReLabel from ImageNet trained model for both methods. The results show that OAMixer+TL outperforms TL for all considered scenarios. Note that the gain of TL is proportional to the model capacity, i.e., more beneficial for the larger model and even harmful for the small model, MobileViT-XXS. We think this is because the additional supervision of TL puts more burden on the models, requiring a larger capacity to digest. In contrast, OAMixer modifies the optimization landscape via reparametrization of patch mixing layers, leading the models to converge to the better optima regardless of the model capacity. Also, note that OAMixer regularizes the overfitting of the vanilla DeiT-B.

Self-supervised learning. Table 3 shows that OAMixer is also effective for self-supervised learning. Here, we apply OAMixer on top of the DINO [11] framework, which are known to effective for learning representations for ViT.

Table 6. Mean average precision (mAP) for multi-object recognition on the COCO dataset. We use the patch-wise object labels, which are given by ReLabel trained on ImageNet. Bold denotes the best results, and parenthesis denotes the gap from the baseline. OAMixer is also effective for recognizing multi-object images.

DeiT-T		DeiT-S	
Baseline	OAMixer (ours)	Baseline	OAMixer (ours)
57.42	59.56 (+2.14)	60.93	62.23 (+1.30)

To this end, we first train the vanilla DINO with DeiT-T on ImageNet. We then train DINO with OAMixer, using the attention map of the pretrained vanilla baseline DINO model as unsupervised binary patch-wise object labels. To evaluate the representation, we train a linear classifier for 9 classes of Background Challenge upon the learned representation. DINO trained with OAMixer learns more object-centric representation, and highly improves the classification accuracy and background robustness.

Generalization on distribution shifts. Table 4 shows the classification accuracy of models trained on ImageNet-9, evaluated on various distribution-shifted datasets: 9 superclass (370 class) subsets of ImageNetV2 [41], ImageNet-Real [6], ImageNet-Rendition [24], ImageNet-Stylized [21], and ImageNet-Sketch [51], denoted by adding ‘-9’ at the suffix of their names. OAMixer also generalizes well on distribution shifts. We use BigBiGAN for object labels since it worked better than ReLabel; finding salient regions is easier than predicting semantics for the unseen samples.

More classification results. Table 5 presents the classification accuracy on various downstream datasets, including CIFAR- $\{10,100\}$ [30], Food-101 [7], and Pets [38]. We modified ViT architectures for CIFAR to use 2×2 patch size following Trockman et al. [48], as CIFAR has a smaller resolution of 32×32 than the original architecture for 224×224 . Here, we compare two versions of OAMixer: ‘‘OAMixer’’ using ReLabel trained on each downstream dataset, and ‘‘OAMixer*’’ using ReLabel trained on ImageNet. We observe that ReLabels trained on the downstream task and ImageNet show comparable performance. We think this is because of the distribution shift on the downstream task, which compensates for the extra data of ImageNet. Thus, one can simply use the ImageNet-pretrained ReLabel instead of training a specific object labeler for each dataset.

Multi-object recognition. Table 6 presents the mean average precision (mAP) results on the COCO multi-object recognition task, which aims to predict the occurrence of each class for multi-object images. Here, we use multi-class prediction maps for OAMixer since binary saliency maps cannot distinguish different objects. Specifically, we use

Table 7. Learned mask scales $\kappa^{(l)}$ over layers.

	Layer 1/4	Layer 2/4	Layer 3/4	Layer 4/4
DeiT-S	1.571	0.783	0.945	0.287
MLP-Mixer-S/16	0.744	0.000	0.001	0.061
ConvMixer-S/16	0.871	2.347	1.498	0.001

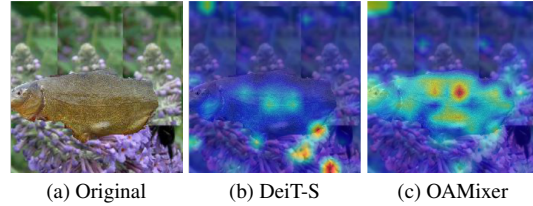


Figure 2. Saliency maps of DeiT-S and OAMixer (ours).

ReLabel from ImageNet trained model. The results confirm that OAMixer is also effective for multi-object images.

4.3. Analysis

Mask scales. We report the mask scales $\kappa^{(l)}$ in Eq. (3) of trained models in Table 7. We divide the model quarterly by depth and average the values for each quarter. Remark that the models set higher $\kappa^{(l)}$ for lower layers and lower $\kappa^{(l)}$ for higher layers (especially $\kappa^{(l)} = 0$ for the final layer), i.e., see the objects first then expand its view, resembling the local-to-global structure of CNNs. ConvMixer sets low $\kappa^{(l)}$ for the early layers since it is hard to understand the objects due to the restricted view of convolution.

Saliency maps. We visualize the saliency maps [12] of DeiT-S and OAMixer on top of it, trained on ImageNet-9. Figure 2 shows the saliency maps on a background-shifted image from the MIXED-RAND dataset, indicating that OAMixer sees a more object-centric view. Quantitatively, OAMixer improves the mean intersection-over-union (mIoU) of saliency maps of DeiT-S by 10% relatively.

5. Conclusion

We propose OAMixer, a novel object-centric framework to refine patch-based models. We demonstrate that OAMixer outperforms the classification and background robustness of various patch-based models. We also show the effectiveness of OAMixer on various downstream tasks. We hope OAMixer could inspire new research directions for patch-based models and object-centric learning.

Acknowledgement

This research was supported by the Engineering Research Center Program through the National Research Foundation of Korea (NRF) funded by the Korean Government MSIT (NRF2018R1A5A1059921).

References

- [1] Samira Abnar, Mostafa Dehghani, Behnam Neyshabur, and Hanie Sedghi. Exploring the limits of large scale pre-training. *arXiv preprint arXiv:2110.02095*, 2021. **1**
- [2] Hassan Akbari, Linagzhe Yuan, Rui Qian, Wei-Hong Chuang, Shih-Fu Chang, Yin Cui, and Boqing Gong. Vatt: Transformers for multimodal self-supervised learning from raw video, audio and text. *arXiv preprint arXiv:2104.11178*, 2021. **1**
- [3] Anurag Arnab, Mostafa Dehghani, Georg Heigold, Chen Sun, Mario Lučić, and Cordelia Schmid. Vivit: A video vision transformer. In *IEEE International Conference on Computer Vision*, 2021. **1**
- [4] Yutong Bai, Jieru Mei, Alan L Yuille, and Cihang Xie. Are transformers more robust than cnns? In *Advances in Neural Information Processing Systems*, 2021. **1**
- [5] Gedas Bertasius, Heng Wang, and Lorenzo Torresani. Is space-time attention all you need for video understanding? In *International Conference on Machine Learning*, 2021. **1**
- [6] Lucas Beyer, Olivier J Hénaff, Alexander Kolesnikov, Xiaoohua Zhai, and Aäron van den Oord. Are we done with imagenet? *arXiv preprint arXiv:2006.07159*, 2020. **8**
- [7] Lukas Bossard, Matthieu Guillaumin, and Luc Van Gool. Food-101—mining discriminative components with random forests. In *European Conference on Computer Vision*, 2014. **8**
- [8] Andrew Brock, Soham De, Samuel L Smith, and Karen Simonyan. High-performance large-scale image recognition without normalization. In *International Conference on Machine Learning*, 2021. **6**
- [9] Andrew Brock, Jeff Donahue, and Karen Simonyan. Large scale gan training for high fidelity natural image synthesis. In *International Conference on Learning Representations*, 2019. **4**
- [10] Tom B Brown, Benjamin Mann, Nick Ryder, Melanie Subbiah, Jared Kaplan, Prafulla Dhariwal, Arvind Neelakantan, Pranav Shyam, Girish Sastry, Amanda Askell, et al. Language models are few-shot learners. In *Advances in Neural Information Processing Systems*, 2020. **2**
- [11] Mathilde Caron, Hugo Touvron, Ishan Misra, Hervé Jégou, Julien Mairal, Piotr Bojanowski, and Armand Joulin. Emerging properties in self-supervised vision transformers. In *IEEE International Conference on Computer Vision*, 2021. **2, 3, 4, 5, 7**
- [12] Hila Chefer, Shir Gur, and Lior Wolf. Transformer interpretability beyond attention visualization. In *IEEE Conference on Computer Vision and Pattern Recognition*, 2021. **3, 4, 8**
- [13] Bowen Cheng, Ishan Misra, Alexander G Schwing, Alexander Kirillov, and Rohit Girdhar. Masked-attention mask transformer for universal image segmentation. *arXiv preprint arXiv:2112.01527*, 2021. **3**
- [14] Jifeng Dai, Kaiming He, and Jian Sun. Convolutional feature masking for joint object and stuff segmentation. In *IEEE Conference on Computer Vision and Pattern Recognition*, 2015. **3**
- [15] Zihang Dai, Hanxiao Liu, Quoc V Le, and Mingxing Tan. Coatnet: Marrying convolution and attention for all data sizes. In *Advances in Neural Information Processing Systems*, 2021. **1, 2, 7**
- [16] Stéphane d’Ascoli, Hugo Touvron, Matthew Leavitt, Ari Morcos, Giulio Biroli, and Levent Sagun. Convit: Improving vision transformers with soft convolutional inductive biases. In *International Conference on Machine Learning*, 2021. **1, 2, 7**
- [17] Jia Deng, Wei Dong, Richard Socher, Li-Jia Li, Kai Li, and Li Fei-Fei. Imagenet: A large-scale hierarchical image database. In *IEEE Conference on Computer Vision and Pattern Recognition*, 2009. **2, 4, 6, 7**
- [18] Jacob Devlin, Ming-Wei Chang, Kenton Lee, and Kristina Toutanova. Bert: Pre-training of deep bidirectional transformers for language understanding. In *Annual Conference of the North American Chapter of the Association for Computational Linguistics*, 2019. **2**
- [19] Alexey Dosovitskiy, Lucas Beyer, Alexander Kolesnikov, Dirk Weissenborn, Xiaoohua Zhai, Thomas Unterthiner, Mostafa Dehghani, Matthias Minderer, Georg Heigold, Sylvain Gelly, et al. An image is worth 16x16 words: Transformers for image recognition at scale. In *International Conference on Learning Representations*, 2021. **1, 2**
- [20] Haoqi Fan, Bo Xiong, Karttikeya Mangalam, Yanghao Li, Zhicheng Yan, Jitendra Malik, and Christoph Feichtenhofer. Multiscale vision transformers. In *IEEE International Conference on Computer Vision*, 2021. **1, 2**
- [21] Robert Geirhos, Patricia Rubisch, Claudio Michaelis, Matthias Bethge, Felix A Wichmann, and Wieland Brendel. Imagenet-trained cnns are biased towards texture; increasing shape bias improves accuracy and robustness. In *International Conference on Learning Representations*, 2019. **8**
- [22] Kaiming He, Xinlei Chen, Saining Xie, Yanghao Li, Piotr Dollár, and Ross Girshick. Masked autoencoders are scalable vision learners. *arXiv preprint arXiv:2111.06377*, 2021. **1**
- [23] Kaiming He, Xiangyu Zhang, Shaoqing Ren, and Jian Sun. Deep residual learning for image recognition. In *IEEE Conference on Computer Vision and Pattern Recognition*, 2016. **6**
- [24] Dan Hendrycks, Steven Basart, Norman Mu, Saurav Kadavath, Frank Wang, Evan Dorundo, Rahul Desai, Tyler Zhu, Samyak Parajuli, Mike Guo, Dawn Song, Jacob Steinhardt, and Justin Gilmer. The many faces of robustness: A critical analysis of out-of-distribution generalization. In *IEEE International Conference on Computer Vision*, 2021. **8**
- [25] Byeongho Heo, Sangdoon Yun, Dongyoon Han, Sanghyuk Chun, Junsuk Choe, and Seong Joon Oh. Rethinking spatial dimensions of vision transformers. In *IEEE International Conference on Computer Vision*, 2021. **1, 2**
- [26] Roei Herzig, Elad Ben-Avraham, Karttikeya Mangalam, Amir Bar, Gal Chechik, Anna Rohrbach, Trevor Darrell, and Amir Globerson. Object-region video transformers. *arXiv preprint arXiv:2110.06915*, 2021. **3**
- [27] Zihang Jiang, Qibin Hou, Li Yuan, Daquan Zhou, Yujun Shi, Xiaojie Jin, Anran Wang, and Jiashi Feng. All tokens matter: Token labeling for training better vision transformers. In *Advances in Neural Information Processing Systems*, 2021. **2, 3, 7**
- [28] Salman Khan, Muzammal Naseer, Munawar Hayat, Syed Waqas Zamir, Fahad Shahbaz Khan, and Mubarak Shah. Transformers in vision: A survey. *arXiv preprint*

- arXiv:2101.01169*, 2021. 1, 2
- [29] Thomas Kipf, Gamaleldin F Elsayed, Aravindh Mahendran, Austin Stone, Sara Sabour, Georg Heigold, Rico Jonschkowski, Alexey Dosovitskiy, and Klaus Greff. Conditional object-centric learning from video. *arXiv preprint arXiv:2111.12594*, 2021. 3
- [30] Alex Krizhevsky, Geoffrey Hinton, et al. Learning multiple layers of features from tiny images. 2009. 8
- [31] Yann LeCun, Léon Bottou, Yoshua Bengio, and Patrick Haffner. Gradient-based learning applied to document recognition. *Proceedings of the IEEE*, 86(11):2278–2324, 1998. 1, 2
- [32] Dongze Lian, Zehao Yu, Xing Sun, and Shenghua Gao. As-mlp: An axial shifted mlp architecture for vision. *arXiv preprint arXiv:2107.08391*, 2021. 1
- [33] Hanxiao Liu, Zihang Dai, David R So, and Quoc V Le. Pay attention to mlps. In *Advances in Neural Information Processing Systems*, 2021. 1
- [34] Ze Liu, Yutong Lin, Yue Cao, Han Hu, Yixuan Wei, Zheng Zhang, Stephen Lin, and Baining Guo. Swin transformer: Hierarchical vision transformer using shifted windows. In *IEEE International Conference on Computer Vision*, 2021. 1, 2
- [35] Francesco Locatello, Dirk Weissenborn, Thomas Unterthiner, Aravindh Mahendran, Georg Heigold, Jakob Uszkoreit, Alexey Dosovitskiy, and Thomas Kipf. Object-centric learning with slot attention. In *Advances in Neural Information Processing Systems*, 2020. 3
- [36] Sangwoo Mo, Hyunwoo Kang, Kihyuk Sohn, Chun-Liang Li, and Jinwoo Shin. Object-aware contrastive learning for debiased scene representation. In *Advances in Neural Information Processing Systems*, 2021. 3, 4
- [37] Muzammal Naseer, Kanchana Ranasinghe, Salman Khan, Munawar Hayat, Fahad Shahbaz Khan, and Ming-Hsuan Yang. Intriguing properties of vision transformers. In *Advances in Neural Information Processing Systems*, 2021. 1
- [38] Omkar M Parkhi, Andrea Vedaldi, Andrew Zisserman, and CV Jawahar. Cats and dogs. In *IEEE Conference on Computer Vision and Pattern Recognition*, 2012. 8
- [39] Sayak Paul and Pin-Yu Chen. Vision transformers are robust learners. In *AAAI Conference on Artificial Intelligence*, 2022. 1
- [40] Alec Radford, Jong Wook Kim, Chris Hallacy, Aditya Ramesh, Gabriel Goh, Sandhini Agarwal, Girish Sastry, Amanda Askell, Pamela Mishkin, Jack Clark, et al. Learning transferable visual models from natural language supervision. In *International Conference on Machine Learning*, 2021. 1
- [41] Benjamin Recht, Rebecca Roelofs, Ludwig Schmidt, and Vaishaal Shankar. Do imagenet classifiers generalize to imagenet? In *International Conference on Machine Learning*, 2019. 8
- [42] Carsten Rother, Vladimir Kolmogorov, and Andrew Blake. ” grabcut” interactive foreground extraction using iterated graph cuts. *ACM transactions on graphics (TOG)*, 23(3):309–314, 2004. 13
- [43] Ramprasaath R Selvaraju, Michael Cogswell, Abhishek Das, Ramakrishna Vedantam, Devi Parikh, and Dhruv Batra. Grad-cam: Visual explanations from deep networks via gradient-based localization. In *IEEE International Conference on Computer Vision*, 2017. 3, 4
- [44] Andreas Steiner, Alexander Kolesnikov, Xiaohua Zhai, Ross Wightman, Jakob Uszkoreit, and Lucas Beyer. How to train your vit? data, augmentation, and regularization in vision transformers. *arXiv preprint arXiv:2106.10270*, 2021. 1, 2
- [45] Ilya Tolstikhin, Neil Houlsby, Alexander Kolesnikov, Lucas Beyer, Xiaohua Zhai, Thomas Unterthiner, Jessica Yung, Daniel Keysers, Jakob Uszkoreit, Mario Lucic, et al. Mlp-mixer: An all-mlp architecture for vision. In *Advances in Neural Information Processing Systems*, 2021. 1, 2, 6
- [46] Hugo Touvron, Piotr Bojanowski, Mathilde Caron, Matthieu Cord, Alaaeldin El-Nouby, Edouard Grave, Gautier Izacard, Armand Joulin, Gabriel Synnaeve, Jakob Verbeek, et al. Resmlp: Feedforward networks for image classification with data-efficient training. *arXiv preprint arXiv:2105.03404*, 2021. 1
- [47] Hugo Touvron, Matthieu Cord, Matthijs Douze, Francisco Massa, Alexandre Sablayrolles, and Hervé Jégou. Training data-efficient image transformers & distillation through attention. In *International Conference on Machine Learning*, 2021. 2, 5
- [48] Asher Trockman and Zico J. Kolter. Patches are all you need? *arXiv preprint arXiv:2201.09792*, 2022. 1, 2, 6, 8, 14
- [49] Ashish Vaswani, Noam Shazeer, Niki Parmar, Jakob Uszkoreit, Llion Jones, Aidan N Gomez, Łukasz Kaiser, and Illia Polosukhin. Attention is all you need. In *Advances in Neural Information Processing Systems*, 2017. 1, 2, 3
- [50] Andrey Voynov, Stanislav Morozov, and Artem Babenko. Object segmentation without labels with large-scale generative models. In *International Conference on Machine Learning*, 2021. 3, 4, 13
- [51] Haohan Wang, Songwei Ge, Zachary Lipton, and Eric P Xing. Learning robust global representations by penalizing local predictive power. In *Advances in Neural Information Processing Systems*, 2019. 8
- [52] Wenhai Wang, Enze Xie, Xiang Li, Deng-Ping Fan, Kaitao Song, Ding Liang, Tong Lu, Ping Luo, and Ling Shao. Pyramid vision transformer: A versatile backbone for dense prediction without convolutions. In *IEEE International Conference on Computer Vision*, 2021. 1, 2
- [53] Haiping Wu, Bin Xiao, Noel Codella, Mengchen Liu, Xiyang Dai, Lu Yuan, and Lei Zhang. Cvt: Introducing convolutions to vision transformers. *arXiv preprint arXiv:2103.15808*, 2021. 1, 2
- [54] Yi-Fu Wu, Jaesik Yoon, and Sungjin Ahn. Generative video transformer: Can objects be the words? In *International Conference on Machine Learning*, 2021. 3
- [55] Kai Xiao, Logan Engstrom, Andrew Ilyas, and Aleksander Madry. Noise or signal: The role of image backgrounds in object recognition. In *International Conference on Learning Representations*, 2021. 6, 12
- [56] Tete Xiao, Piotr Dollar, Mannat Singh, Eric Mintun, Trevor Darrell, and Ross Girshick. Early convolutions help transformers see better. In *Advances in Neural Information Processing Systems*, 2021. 1, 2
- [57] Weihao Yu, Mi Luo, Pan Zhou, Chenyang Si, Yichen Zhou, Xinchao Wang, Jiashi Feng, and Shuicheng Yan. Metaformer is actually what you need for vision. *arXiv*

- preprint arXiv:2111.11418*, 2021. [1](#), [2](#)
- [58] Kun Yuan, Shaopeng Guo, Ziwei Liu, Aojun Zhou, Fengwei Yu, and Wei Wu. Incorporating convolution designs into visual transformers. In *IEEE International Conference on Computer Vision*, 2021. [1](#), [2](#)
- [59] Li Yuan, Yunpeng Chen, Tao Wang, Weihao Yu, Yujun Shi, Zihang Jiang, Francis EH Tay, Jiashi Feng, and Shuicheng Yan. Tokens-to-token vit: Training vision transformers from scratch on imagenet. In *IEEE International Conference on Computer Vision*, 2021. [1](#), [2](#)
- [60] Sangdoon Yun, Seong Joon Oh, Byeongho Heo, Dongyoon Han, Junsuk Choe, and Sanghyuk Chun. Re-labeling imagenet: from single to multi-labels, from global to localized labels. In *IEEE Conference on Computer Vision and Pattern Recognition*, 2021. [3](#), [5](#), [13](#)
- [61] Xiaohua Zhai, Alexander Kolesnikov, Neil Houlsby, and Lucas Beyer. Scaling vision transformers. *arXiv preprint arXiv:2106.04560*, 2021. [1](#)

A. Discussions on Background Challenge

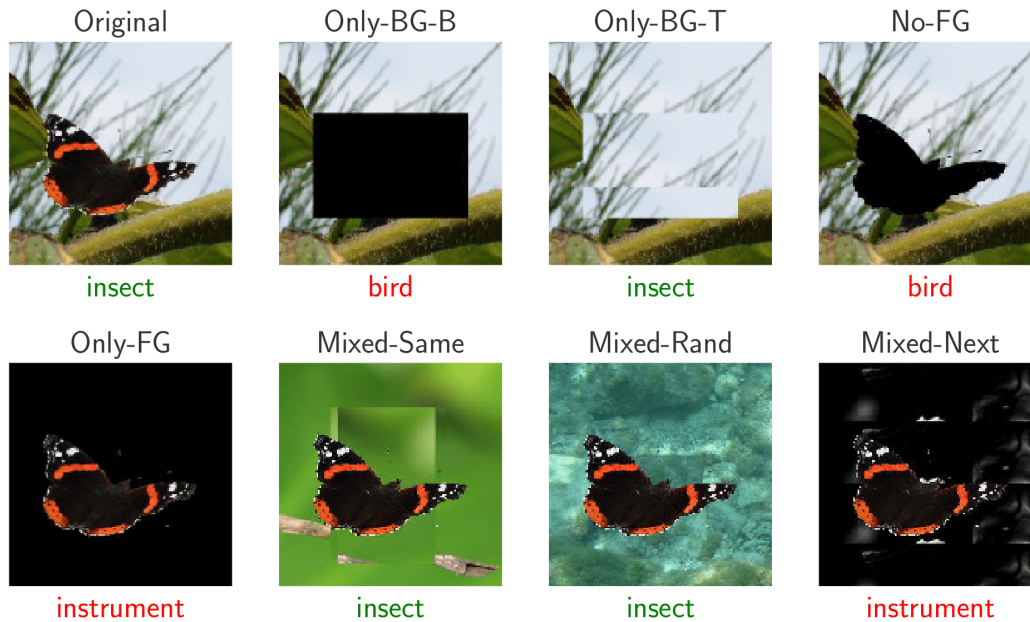


Figure 3. Datasets in the Background Challenge benchmark.

Figure 3 visualizes the datasets in the Background Challenge [55] benchmark, which provides various combinations of foregrounds and backgrounds: ORIGINAL (\uparrow), ONLY-BG-B (\downarrow), ONLY-BG-T (\downarrow), NO-FG (\downarrow), ONLY-FG (\uparrow), MIXED-SAME (\uparrow), MIXED-RAND (\uparrow), MIXED-NEXT (\uparrow). The upper or lower arrows indicate whether the model should predict the class well or not, respectively. We omit ONLY-BG-T, NO-FG, ONLY-FG, and MIXED-NEXT results due to the brevity of the presentation. Nevertheless, we provide some observations and discussions on them:

- ONLY-FG and MIXED-NEXT shows the same trend of MIXED-RAND.
- NO-FG is controversial to be predicted or not since the image contains the shadow of the object.
- ONLY-BG-T increases when ORIGINAL increases. However, OAMixer only increases ONLY-BG-T a little while ORIGINAL a lot compared to the baselines.

B. OAMixer using different object labels

Table 8. Comparison of OAMixer using various object labels. We test three different object labels: (a) BigBiGAN [50] (unsupervised binary saliency map), (b) ReLabel [60] (weakly-supervised multi-class map) and (c) Bbox + Grabcut [42] (binary saliency map extracted from the ground-truth bounding box). We report the classification accuracy (\uparrow) and background robustness (\downarrow), where higher and lower values are better for each metric. ‘+’ denotes the modules added to the baseline (not accumulated), and parenthesis denotes the gap from the baseline. The table shows OAMixer consistently outperforms the baseline for all considering object labelers.

	Object label	Original (\uparrow)	Only-BG-B (\downarrow)	Mixed-Same (\uparrow)	Mixed-Rand (\uparrow)	BG-Gap (\downarrow)
DeiT-T	-	70.62	35.48	63.31	39.56	23.75
+ OAMixer (ours)	BigBiGAN	80.15 (+9.53)	32.37 (-3.11)	71.98 (+8.66)	48.77 (+9.21)	23.21 (-0.54)
+ OAMixer (ours)	ReLabel	81.98 (+11.36)	30.89 (-4.59)	73.38 (+10.07)	51.53 (+11.97)	21.85 (-1.90)
+ OAMixer (ours)	Bbox+GrabCut	83.23 (+12.61)	34.49 (-0.99)	74.32 (+11.01)	52.77 (+13.21)	21.55 (-2.20)
DeiT-S	-	82.69	39.46	73.88	50.49	23.39
+ OAMixer (ours)	BigBiGAN	83.88 (+1.19)	36.59 (-2.87)	75.95 (+2.07)	54.07 (+3.58)	21.88 (-1.51)
+ OAMixer (ours)	ReLabel	86.32 (+3.63)	31.78 (-7.68)	78.44 (+4.56)	56.74 (+6.25)	21.70 (-1.69)
+ OAMixer (ours)	Bbox+GrabCut	87.04 (+4.35)	37.80 (-1.66)	78.15 (+4.27)	57.80 (+7.31)	20.35 (-3.04)
MLP-Mixer-S/16	-	84.99	40.96	76.52	54.72	21.80
+ OAMixer (ours)	BigBiGAN	86.30 (+1.31)	36.64 (-4.32)	78.47 (+1.95)	58.54 (+3.82)	19.93 (-1.87)
+ OAMixer (ours)	ReLabel	87.68 (+2.69)	27.28 (-13.68)	79.43 (+2.91)	60.44 (+5.72)	18.99 (-2.81)
+ OAMixer (ours)	Bbox+GrabCut	88.32 (+3.33)	37.51 (-3.45)	79.68 (+3.16)	61.85 (+7.13)	17.83 (-3.97)
ConvMixer-S/16	-	86.32	41.38	78.59	56.99	21.60
+ OAMixer (ours)	BigBiGAN	86.35 (+0.03)	37.09 (-4.29)	80.27 (+1.68)	59.19 (+2.20)	21.09 (-0.51)
+ OAMixer (ours)	ReLabel	88.49 (+2.17)	35.60 (-5.78)	81.70 (+3.11)	63.93 (+6.94)	17.77 (-3.83)
+ OAMixer (ours)	Bbox+GrabCut	87.73 (+1.41)	34.64 (-6.74)	80.03 (+1.44)	61.88 (+4.89)	18.15 (-3.45)

Table 8 compares OAMixer using BigBiGAN and ReLabel. We also compare with Bbox+Grabcut, a binary saliency map extracted from the bounding boxes using the GrabCut [42] algorithm, which is provided by the Background Challenge benchmark. Bbox+GrabCut gives accurate object masks as it leverages the bounding boxes. Here, one can see the differences between object labels. First, Bbox+GrabCut performs the best for most cases, supporting that the accurate object labels are helpful for OAMixer. Second, ReLabel performs the best for the ONLY-BG-B dataset; this is because the binary saliency models predict the background-only images as all-zero values, reducing OAMixer behaves like the vanilla patch-based model. We use ReLabel as a default choice in our experiments, as it does not require additional human annotations yet performs well.

C. ReMixer using ReLabel from ImageNet-9

Table 9. Background Challenge results of ReMixer using ReLabel trained on ImageNet-9 (IN-9) and ImageNet (IN-1K). ReLabel trained on IN-9 shows similar trend with IN-1K.

	ReLabel	Original (\uparrow)	Only-BG-B (\downarrow)	Mixed-Same (\uparrow)	Mixed-Rand (\uparrow)	BG-Gap (\downarrow)
DeiT-T		70.62	35.48	63.31	39.56	23.75
+ ReMixer (ours)	IN-9	79.26 (+8.64)	33.63 (-1.85)	70.94 (+7.63)	47.38 (+7.82)	23.56 (-0.19)
+ ReMixer (ours)	IN-1K	81.98 (+11.36)	30.89 (-4.59)	73.38 (+10.07)	51.53 (+11.97)	21.85 (-1.90)

Table 9 compares ReMixer using ReLabel trained on ImageNet-9 (IN-9) and ImageNet (IN-1K). ReLabel trained on IN-1K performs better but shows the same trends with IN-9.

D. ImageNet-9 Large (IN-9L) results

Table 10. Background Challenge results of models trained on IN-9 and IN-9L datasets. While training on IN-9L significantly improves the performance overall, it shows a consistent trend with IN-9.

	Original (↑)	Only-BG-B (↓)	Mixed-Same (↑)	Mixed-Rand (↑)	BG-Gap (↓)
<i>Trained on IN-9</i>					
DeiT-T	70.62	35.48	47.04	39.56	23.75
+ ReMixer (ours)	81.98 (+11.36)	30.89 (-4.59)	54.03 (+6.99)	51.53 (+11.97)	21.85 (-1.90)
<i>Trained on IN-9L</i>					
DeiT-T	93.38	41.93	77.75	68.15	17.21
+ ReMixer (ours)	95.31 (+1.93)	32.32 (-9.61)	81.16 (+3.41)	74.44 (+6.29)	14.00 (-3.21)

Table 10 compares the models trained on ImageNet-9 (IN-9) and the larger version of IN-9 (IN-9L). The models trained on IN-9L performs better but shows the same trends with IN-9.

E. Sharing weights for ConvMixer

Table 11. Comparison of ConvMixer sharing (white line) and not sharing (gray line) kernels over channels. We add ‘-Full’ to denote the latter, which uses $\times D$ parameters for patch mixing layers where D is the number of channels. ConvMixer + OAMixer is comparable with ConvMixer-Full.

	Original (↑)	Only-BG-B (↓)	Mixed-Same (↑)	Mixed-Rand (↑)	BG-Gap (↓)
ConvMixer-S/16	86.32	41.38	66.84	56.99	21.60
+ OAMixer (ours)	88.49 (+2.17)	35.60 (-5.78)	71.60 (+4.76)	63.93 (+6.94)	17.77 (-3.83)
ConvMixer-S/16-Full	88.67 (+2.35)	40.20 (-1.18)	70.72 (+3.88)	62.84 (+5.85)	18.47 (-3.13)

We adopt ConvMixer [48] to share the convolution kernels over channels to reduce memory and computation in our experiments. Table 11 shows the comparison of our adopted ConvMixer and the original one (ConvMixer-Full). ConvMixer + OAMixer is comparable or even outperforms ConvMixer-Full, yet using $D = 512$ times smaller parameters for patch mixing layers.